A fractional step θ-method for viscoelastic fluid flow using a SUPG approximation

J.C. Chrispell [*] V.J. Ervin [†] E.W. Jenkins [*]

October 26, 2007

Abstract

In this article a fractional step θ-method is described and studied for the approximation of time dependent viscoelastic fluid flow equations, using the Johnson-Segalman constitutive model. The θ-method implementation allows the velocity and pressure approximations to be decoupled from the stress, reducing the number of unknowns resolved at each step of the method. The constitutive equation is stabilized using a Streamline Upwinded Petrov-Galerkin (SUPG)-method. A priori error estimates are given for the approximation scheme. Numerical computations supporting the theoretical results and demonstrating the θ-method are also presented.

Key words. θ-method; splitting method; viscoelastic flow

AMS Mathematics subject classifications. 65N30

1 Introduction

Numerical methods for modeling viscoelastic fluid flow are difficult for a variety of reasons. The modeling equations (assuming *slow* flow) represent a "Stokes system" for the conservation of mass and momentum equations, coupled with a non-linear hyperbolic equation describing the constitutive equation for the stress. The numerical approximation requires the determination of the fluid's velocity, pressure and stress (a symmetric tensor). For an accurate approximation a direct approximation technique requires the solution of a very large nonlinear system of equations at each time step.

The fractional step θ-method [26, 24, 25] decouples the approximation of velocity and pressure from the approximation of the stress, thereby reducing the size of the algebraic systems which have to be solved at each sub-step. An added benefit of the θ-method [26] is that the algebraic systems to be solved at each substep are linear.

[*]Department of Mathematical Sciences, Clemson University, Clemson, SC 29634-0975, USA. This work was supported in part by the National Science Foundation under Award Number DMS-0410792, and U.S. Army Research Office Grant W911NF-05-1-0380. E-mail addresses: jchrisp@clemson.edu (J.C. Chrispell), lea@clemson.edu (E.W. Jenkins).

[†]Department of Mathematical Sciences, Clemson University, Clemson, SC 29634-0975, USA. This work was supported in part by the National Science Foundation under Award Number DMS-0410792. Corresponding author. E-mail address: vjervin@clemson.edu (V.J. Ervin)

The fractional step θ-method was introduced, and its temporal approximation accuracy studied for a symmetric, positive definite spatial operator, by Glowinski and Périaux in [12]. The method is widely used for the accurate approximation of the Navier-Stokes equations (NSE) [27, 28, 15]. In [16], Kloucek and Rys showed, assuming a unique solution existed, that the θ-method approximation converged to the solution of the NSE as the spatial and mesh parameters went to zero (h, $\Delta t \rightarrow 0_+$). The temporal discretization error for the θ-method for the NSE was studied by Müller-Urbaniak in [19] and shown to be second order. In [7] the θ-method applied to convection-diffusion equations was shown to be second order in time.

The implementation of the fractional step θ-method in [26] for viscoelasticity differs significantly from that for the NSE. For the NSE at each sub-step the discretization contains the *stabilizing* operator $-\Delta \mathbf{u}$. For the viscoelasticity problem the middle substep is a pure convection (transport) problem that requires stabilization in order to control the creation of spurious oscillations in the numerical approximation. Marchal and Crochet [18] were the first to use streamline upwinding to stabilize the hyperbolic constitutive equation in viscoelastic flow. A second common approach to stabilizing the convective transport problem is to use a discontinuous Galerkin (DG) approximation for the stress [2, 1].

Error analysis of finite element approximations to steady state viscoelastic flow was first done by Baranger and Sandri in [2] using a DG formulation of the constitutive equation. In [23] Sandri presented analysis of the steady state problem using a streamline upwind Petrov-Galerkin (SUPG) method of stabilization. The time-dependent problem was first analyzed by Baranger and Wardi in [3], using an implict Euler temporal discretization and DG approximation for the hyperbolic constitutive equation. Ervin and Miles analyzed the problem using an implicit Euler time discretization and a SUPG discretization for the stress in [10]. Analysis of a modified Euler-SUPG approximation to the transient viscoelastic flow problem was presented by Bensaada and Esselaoui in [4]. The temporal accuracy of the approximation schemes studied in [3, 4, 10] are all $O(\Delta t)$. Ervin and Heuer proposed a Crank-Nicolson time discretization method [9] which they showed was $O\left((\Delta t^2)\right)$. Their method uses a three level scheme to approximate the nonlinear terms in the equations. Consequently their approximation algorithm only requires linear systems of equations be solved.

In this article we analyze a fractional step θ-method for the approximation of viscoelastic fluid flows. Advantages of the method are threefold: (i) second order accuracy with respect to the temporal discretization, (ii) only linear systems of equations need to be solved, (iii) the linear systems to be solved only involve the velocity-pressure or the stress unknowns (resulting in smaller linear systems).

This paper is organized as follows. In the next section we specify the problem and describe the fractional step θ-method for the viscoelastic modeling equations. In Section 3 the mathematical notation used is given. In Section 4 we show computability of the algorithm, and present the a priori error estimates that support the method. Two numerical examples demonstrating the method are presented in Section 5.

2 The Mathematical Model and θ-Method Approximation

In this section we present the modeling equations for viscoelastic fluid flow as well as a fractional step θ-method approximation scheme. Following the description of the θ-method, several definitions used to formulate the problem in an appropriate mathematical setting are given.

2.1 Modeling Equations

The non-dimensional modeling equations for a viscoelastic fluid in a given domain $\Omega \subset \mathbb{R}^{\acute{d}}$ ($\acute{d} = 2, 3$) using a Johnson-Segalman constitutive equation are written as:

$$
\begin{aligned}
\boldsymbol{\sigma} + \lambda \left(\frac{\partial \boldsymbol{\sigma}}{\partial t} + \boldsymbol{u} \cdot \nabla \boldsymbol{\sigma} + g_a(\boldsymbol{\sigma}, \nabla \boldsymbol{u}) \right) - 2\alpha \mathbf{d}(\boldsymbol{u}) &= \mathbf{0} \;\text{ in } \Omega, && (2.1)\\
Re \left(\frac{\partial \boldsymbol{u}}{\partial t} + \boldsymbol{u} \cdot \nabla \boldsymbol{u} \right) + \nabla p - 2(1-\alpha) \nabla \cdot \mathbf{d}(\boldsymbol{u}) - \nabla \cdot \boldsymbol{\sigma} &= \mathbf{f} \;\text{ in } \Omega, && (2.2)\\
\nabla \cdot \boldsymbol{u} &= 0 \;\text{ in } \Omega, && (2.3)\\
\boldsymbol{u} &= \mathbf{0} \;\text{ on } \partial\Omega, && (2.4)\\
\boldsymbol{u}(0, x) &= \boldsymbol{u}_0(x) \text{ in } \Omega, && (2.5)\\
\boldsymbol{\sigma}(0, x) &= \boldsymbol{\sigma}_0(x) \text{ in } \Omega. && (2.6)
\end{aligned}
$$

Here (2.1) is the constitutive equation relating the fluids velocity $\boldsymbol{u}$ to the stress $\boldsymbol{\sigma}$, and (2.2) and (2.3) are the conservation of momentum and conservation of mass equations. The fluid pressure is denoted by p. The Weissenberg number λ is a dimensionless constant defined as the product of a characteristic strain rate and the relaxation time of the fluid [5]. Re denotes the fluids Reynolds number, $\mathbf{f}$ are the body forces acting on the fluid, and $\alpha \in (0, 1)$ denotes the fraction of the total viscosity that is viscoelastic.

The term g_a and deformation tensor $\mathbf{d}(\boldsymbol{u})$ are defined as:

$$
g_a(\boldsymbol{\sigma}, \nabla \boldsymbol{u}) := \frac{1-a}{2} \left(\boldsymbol{\sigma} \nabla \boldsymbol{u} + (\nabla \boldsymbol{u})^T \boldsymbol{\sigma} \right) - \frac{1+a}{2} \left(\nabla \boldsymbol{u} \boldsymbol{\sigma} + \boldsymbol{\sigma} (\nabla \boldsymbol{u})^T \right)
$$

and

$$
\mathbf{d}(\boldsymbol{u}) = \frac{1}{2} \left(\nabla \boldsymbol{u} + (\nabla \boldsymbol{u})^T \right).
$$

The gradient of $\boldsymbol{u}$ is defined such that $(\nabla \boldsymbol{u})_{i,j} = \partial u_i / \partial x_j$. For the remainder of the paper slow or inertialess flow is assumed, allowing the term $\boldsymbol{u} \cdot \nabla \boldsymbol{u}$ in (2.2) to be ignored. Note that when the parameter $a = 1$ in $g_a(\boldsymbol{\sigma}, \nabla \boldsymbol{u})$ an Oldroyd B constitutive model is obtained. For existence and uniqueness of solutions to (2.1)-(2.6) see [22, 13, 11].

2.2 θ-method

In order to implement a fractional step θ-method for the viscoelastic flow equations, an additive decomposition is used for equations (2.1) and (2.2). Here we introduce a splitting parameter $\omega \in (0, 1)$, and define:

Constitutive equation:

$$
\begin{aligned}
{}_1G_{\boldsymbol{\sigma}} &:= \omega \boldsymbol{\sigma}, && (2.7)\\
{}_2G_{\boldsymbol{\sigma}} &:= (1-\omega)\boldsymbol{\sigma} + \lambda \left(\boldsymbol{u} \cdot \nabla \boldsymbol{\sigma} + g_a(\boldsymbol{\sigma}, \nabla \boldsymbol{u}) \right) - 2\alpha \mathbf{d}(\boldsymbol{u}). && (2.8)
\end{aligned}
$$

Conservation of Momentum:

$$
\begin{aligned}
{}_1F_{\boldsymbol{u}} &:= -2(1-\alpha)\nabla\cdot\mathbf{d}(\boldsymbol{u}) - \nabla\cdot\boldsymbol{\sigma} - \mathbf{f}, && (2.9)\\
{}_2F_{\boldsymbol{u}} &:= 0. && (2.10)
\end{aligned}
$$

Let Δt denote the temporal increment between times t^n and t^{n+1}, and for $c \in \{\theta, \omega, a, \alpha\}$ let $\tilde{c} := 1 - c$. Also, let $f^{(n)} := f(\cdot, n\Delta t)$.

The θ-method approximation for viscoelasticity may then be described as follows. (See also [26, 24]).

θ-Method Algorithm for Viscoelasticity

Step 1a: (Update the stress.)

$$\lambda\frac{\boldsymbol{\sigma}^{(n+\theta)} - \boldsymbol{\sigma}^{(n)}}{\theta\Delta t} + {}_1G_{\boldsymbol{\sigma}}{}^{(n+\theta)} = -{}_2G_{\boldsymbol{\sigma}}{}^{(n)}.$$

Step 1b: (Solve for velocity and pressure.)

$$
\begin{aligned}
Re\frac{\boldsymbol{u}^{(n+\theta)} - \boldsymbol{u}^{(n)}}{\theta\Delta t} + \nabla p^{(n+\theta)} + {}_1F_{\boldsymbol{u}}{}^{(n+\theta)} &= -{}_2F_{\boldsymbol{u}}{}^{(n)},\\
\nabla\cdot\boldsymbol{u}^{(n+\theta)} &= 0.
\end{aligned}
$$

Step 2a: (Update the velocity and pressure.)

$$
\begin{aligned}
Re\frac{\boldsymbol{u}^{\left(n+\tilde{\theta}\right)} - \boldsymbol{u}^{(n+\theta)}}{(1-2\theta)\,\Delta t} + \nabla p^{\left(n+\tilde{\theta}\right)} + {}_2F_{\boldsymbol{u}}{}^{\left(n+\tilde{\theta}\right)} &= -{}_1F_{\boldsymbol{u}}{}^{(n+\theta)},\\
\nabla\cdot\boldsymbol{u}^{\left(n+\tilde{\theta}\right)} &= 0.
\end{aligned}
$$

Step 2b: (Solve for the stress.)

$$\lambda\frac{\boldsymbol{\sigma}^{\left(n+\tilde{\theta}\right)} - \boldsymbol{\sigma}^{(n+\theta)}}{(1-2\theta)\,\Delta t} + {}_2G_{\boldsymbol{\sigma}}{}^{\left(n+\tilde{\theta}\right)} = -{}_1G_{\boldsymbol{\sigma}}{}^{(n+\theta)}.$$

Step 3a and Step 3b: In order to complete the temporal advancement to time t_{n+1}, Step 1a, and Step 1b are repeated with (n) and $(n+\theta)$ replaced by $\left(n+\tilde{\theta}\right)$ and $(n+1)$ respectively.

Note: Due to the chosen decomposition of the constitutive and conservation of momentum equations, (2.7)-(2.10), the approximation of the nonlinear system (2.1)-(2.6) using the θ-method only requires linear systems of equations to be solved at each step in the process.

3 Mathematical Notation

The $L^2(\Omega)$ inner product and norm are denoted by $(\cdot,\cdot)$, and $\|u\|$ respectively. The Sobolev $W_p^k(\Omega)$ norms are denoted by $\|\cdot\|_{W_p^k}$. We use H^k to represent the Sobolev space W_2^k, and $\|\cdot\|_k$ to denote the norm in H^k. Function spaces used in the analysis are:

$$
\begin{aligned}
X &:= H_0^1(\Omega) := \left\{ \boldsymbol{u} \in H^1(\Omega) : \boldsymbol{u} = 0 \text{ on } \partial\Omega \right\}, \\
S &:= \left\{ \boldsymbol{\sigma} = (\sigma_{ij}) : \sigma_{ij} = \sigma_{ji}; \sigma_{ij} \in L^2(\Omega); 1 \le i,j \le \acute{d} \right\} \\
&\qquad \cap \left\{ \boldsymbol{\sigma} = (\sigma_{ij}) : \boldsymbol{u} \cdot \nabla \boldsymbol{\sigma} \in L^2(\Omega),\ \forall \boldsymbol{u} \in X \right\}, \\
Q &:= L_0^2(\Omega) = \left\{ q \in L^2(\Omega) : \int_\Omega q\, dx = 0 \right\}, \\
Z &:= \left\{ \mathbf{v} \in X : \int_\Omega q(\nabla \cdot \mathbf{v})\, dx = 0,\ \ \forall q \in Q \right\}.
\end{aligned}
$$

Recall that the spaces X and Q satisfy the *inf-sup* condition

$$
\inf_{q \in Q} \sup_{\mathbf{v} \in X} \frac{(q, \nabla \cdot \mathbf{v})}{\|q\|\, \|\mathbf{v}\|_1} \ge \beta > 0. \tag{3.1}
$$

A variational formulation of (2.1)-(2.3), found by multiplication of the modeling equations by test functions and integrating over Ω, is: *Find* $(\boldsymbol{u}, \boldsymbol{\sigma}, p) : (0,T] \to X \times S \times Q$ *such that*

$$
\begin{aligned}
\lambda \left(\frac{\partial \boldsymbol{\sigma}}{\partial t}, \boldsymbol{\tau} \right) + (\boldsymbol{\sigma}, \boldsymbol{\tau}) - 2\alpha\, (\mathbf{d}(\boldsymbol{u}), \boldsymbol{\tau}) + \lambda\, (\boldsymbol{u} \cdot \nabla \boldsymbol{\sigma} + g_a(\boldsymbol{\sigma}, \nabla \boldsymbol{u}), \boldsymbol{\tau}) &= 0,\ \ \forall\, \boldsymbol{\tau} \in S, && (3.2) \\
Re \left(\frac{\partial \boldsymbol{u}}{\partial t}, \mathbf{v} \right) - (p, \nabla \cdot \mathbf{v}) + 2(1-\alpha)\, (\mathbf{d}(\boldsymbol{u}), \mathbf{d}(\mathbf{v})) + (\boldsymbol{\sigma}, \mathbf{d}(\mathbf{v})) &= (\mathbf{f}, \mathbf{v}),\ \ \forall\, \mathbf{v} \in X, && (3.3) \\
(\nabla \cdot \boldsymbol{u}, q) &= 0,\ \ \forall\, q \in Q, && (3.4) \\
\boldsymbol{u}(0,x) &= \boldsymbol{u}_0(x), && (3.5) \\
\boldsymbol{\sigma}(0,x) &= \boldsymbol{\sigma}_0(x). && (3.6)
\end{aligned}
$$

As the velocity and pressure spaces X and Q satisfy the inf-sup condition (3.1), an equivalent variational formulation to (3.2)-(3.4) is given by: *Find* $(\boldsymbol{u}, \boldsymbol{\sigma}) : (0,T] \to Z \times S$ *such that*

$$
\begin{aligned}
\lambda \left(\frac{\partial \boldsymbol{\sigma}}{\partial t}, \boldsymbol{\tau} \right) + (\boldsymbol{\sigma}, \boldsymbol{\tau}) - 2\alpha\, (\mathbf{d}(\boldsymbol{u}), \boldsymbol{\tau}) + \lambda\, (\boldsymbol{u} \cdot \nabla \boldsymbol{\sigma} + g_a(\boldsymbol{\sigma}, \nabla \boldsymbol{u}), \boldsymbol{\tau}) &= 0,\ \ \forall\, \boldsymbol{\tau} \in S, && (3.7) \\
Re \left(\frac{\partial \boldsymbol{u}}{\partial t}, \mathbf{v} \right) + 2(1-\alpha)\, (\mathbf{d}(\boldsymbol{u}), \mathbf{d}(\mathbf{v})) + (\boldsymbol{\sigma}, \mathbf{d}(\mathbf{v})) &= (\mathbf{f}, \mathbf{v}),\ \ \forall\, \mathbf{v} \in Z, && (3.8) \\
\boldsymbol{u}(0,x) &= \boldsymbol{u}_0(x), && (3.9) \\
\boldsymbol{\sigma}(0,x) &= \boldsymbol{\sigma}_0(x). && (3.10)
\end{aligned}
$$

To describe the finite element framework let T_h be a triangulation of the discretized domain $\Omega \subset \mathbb{R}^{\acute{d}}$. Then

$$
\bar{\Omega} = \cup K, \ \ K \in T_h.
$$

We assume that there exist constants c_1 and c_2 such that

$$
c_1 h \le h_K \le c_2 \rho_K,
$$

where h_k is the diameter of triangle K, ρ_K is the diameter of the greatest ball (sphere) included in K, and $h = \max_{k \in T_h} h_K$. Let $P_k(A)$ denote the space of polynomials on A of degree no greater than k and $C(\bar{\Omega})^{\acute{d}}$ the space of vector valued functions with $\acute{d}$ components which are continuous on $\bar{\Omega}$. Then the associated finite element spaces are defined by:

$$\begin{aligned}
X_h &:= \left\{\mathbf{v} \in X \cap C(\bar{\Omega})^{\acute{d}} : \mathbf{v}\big|_K \in P_k(K)\, \forall\, K \in T_h\right\}, \\
S_h &:= \left\{\boldsymbol{\tau} \in S \cap C(\bar{\Omega})^{\acute{d}\times\acute{d}} : \boldsymbol{\tau}\big|_K \in P_m(K)\, \forall\, K \in T_h\right\}, \\
Q_h &:= \left\{q \in Q \cap C(\bar{\Omega}) : q\big|_K \in P_q(K)\, \forall\, K \in T_h\right\}, \\
Z_h &:= \left\{\mathbf{v} \in X_h : (q, \nabla\cdot\mathbf{v}) = 0\, \forall\, q \in Q_h\right\}.
\end{aligned}$$

Analogically to the continuous spaces assume that X_h and Q_h satisfy the discrete *inf-sup* condition:

$$\inf_{q\in Q_h} \sup_{\mathbf{v}\in X_h} \frac{(q, \nabla\cdot\mathbf{v})}{\|q\|\,\|\mathbf{v}\|_1} \geq \beta > 0. \tag{3.11}$$

Let $\mathcal{U}$ and $\mathcal{S}$ denote the L^2 projections of $\boldsymbol{u}$ and $\boldsymbol{\sigma}$ onto Z_h and S_h, respectively, and define:

$$\begin{aligned}
\boldsymbol{\Lambda}^{(n)} &= \boldsymbol{u}^{(n)} - \mathcal{U}^{(n)}, & \boldsymbol{E}^{(n)} &= \mathcal{U}^{(n)} - \boldsymbol{u}_h^{(n)}, \\
\boldsymbol{\Gamma}^{(n)} &= \boldsymbol{\sigma}^{(n)} - \mathcal{S}^{(n)}, & \boldsymbol{F}^{(n)} &= \mathcal{S}^{(n)} - \boldsymbol{\sigma}_h^{(n)}, \\
e_{\boldsymbol{u}}^{(n)} &= \boldsymbol{u}^{(n)} - \boldsymbol{u}_h^{(n)}, & e_{\boldsymbol{\sigma}}^{(n)} &= \boldsymbol{\sigma}^{(n)} - \boldsymbol{\sigma}_h^{(n)}.
\end{aligned}$$

We define the discrete temporal operator

$$d_t f^{(n+1)} := \frac{f(t_{n+1}) - f(t_n)}{\Delta t}.$$

When $v(\mathbf{x}, t)$ is defined on the entire time interval $(0, T)$,

$$\|v\|_{\infty,k} := \sup_{0<t<T} \|v(\cdot,t)\|_k\,, \quad \|v\|_{0,k} := \left(\int_0^T \|v(\cdot,t)\|_k^2\, dt\right)^{1/2}, \quad \|v\|(t) := \|v(\cdot,t)\|\,.$$

The following discrete norms are used:

$$|||v|||_{\infty,k} := \max_{1\leq n\leq N} \left\|v^{(n)}\right\|_k, \qquad |||v|||_{0,k} := \left(\sum_{n=1}^{N} \Delta t \left\|v^{(n)}\right\|_k^2\right)^{\frac{1}{2}}.$$

4 Analysis

In this section we investigate the numerical approximation method corresponding to (3.7)-(3.10) First the discrete variational formulation of the θ-method is given. Then computability of the algorithm is shown and a priori error estimates given.

4.1 Discrete Variational Approximation

To stabilize the constitutive equation a streamline upwind Petrov-Galerkin (SUPG) discretization is used to control spurious oscillations in the approximation. This is implemented by testing all terms in the constitutive equation (except the discretized temporal derivative) against modified test elements of the form $\boldsymbol{\tau}_\delta^{(n)}$ where

$$\boldsymbol{\tau}_\delta^{(n)} := \boldsymbol{\tau} + \delta \boldsymbol{u}_h^{(n)} \cdot \nabla \boldsymbol{\tau}. \tag{4.1}$$

Note that if δ is set to zero the standard Galerkin method is obtained. The variational formulations for the steps in the θ-method approximation are as follows.

Step 1a: Find $\boldsymbol{\sigma}_h^{(n+\theta)} \in S_h$ such that

$$\begin{aligned}\frac{\lambda}{\theta\Delta t}\left(\boldsymbol{\sigma}_h^{(n+\theta)}, \boldsymbol{\tau}\right) + \omega\left(\boldsymbol{\sigma}_h^{(n+\theta)}, \boldsymbol{\tau}_\delta^{(n)}\right) = \frac{\lambda}{\theta\Delta t}\left(\boldsymbol{\sigma}_h^{(n)}, \boldsymbol{\tau}\right) - (1-\omega)\left(\boldsymbol{\sigma}_h^{(n)}, \boldsymbol{\tau}_\delta^{(n)}\right) - \lambda\left(\boldsymbol{u}_h^{(n)} \cdot \nabla\boldsymbol{\sigma}_h^{(n)}, \boldsymbol{\tau}_\delta^{(n)}\right) \\ - \lambda\left(g_a(\boldsymbol{\sigma}_h^n, \nabla\boldsymbol{u}_h^{(n)}), \boldsymbol{\tau}_\delta^{(n)}\right) + 2\alpha\left(\mathbf{d}(\boldsymbol{u}_h^{(n)}), \boldsymbol{\tau}_\delta^{(n)}\right), \qquad \forall\, \boldsymbol{\tau} \in S_h.\end{aligned} \tag{4.2}$$

Step 1b: Find $\boldsymbol{u}_h^{(n+\theta)} \in Z_h$ such that

$$\begin{aligned}\frac{Re}{\theta\Delta t}\left(\boldsymbol{u}_h^{(n+\theta)}, \mathbf{v}\right) + 2(1-\alpha)\left(\mathbf{d}(\boldsymbol{u}_h^{(n+\theta)}), \mathbf{d}(\mathbf{v})\right) \\ = \frac{Re}{\theta\Delta t}\left(\boldsymbol{u}_h^{(n)}, \mathbf{v}\right) + \left(\mathbf{f}^{(n+\theta)}, \mathbf{v}\right) - \left(\boldsymbol{\sigma}_h^{(n+\theta)}, \mathbf{d}(\mathbf{v})\right), \qquad \forall\, \mathbf{v} \in Z_h.\end{aligned} \tag{4.3}$$

Step 2a: Find $u_h^{(n+\tilde{\theta})} \in Z_h$ such that

$$\begin{aligned}\frac{Re}{(1-2\theta)\Delta t}\left(\boldsymbol{u}_h^{(n+\tilde{\theta})}, \mathbf{v}\right) = \frac{Re}{(1-2\theta)\Delta t}\left(\boldsymbol{u}_h^{(n+\theta)}, \mathbf{v}\right) \\ - 2(1-\alpha)\left(\mathbf{d}(\boldsymbol{u}_h^{(n+\theta)}), \mathbf{d}(\mathbf{v})\right) + \left(\mathbf{f}^{(n+\theta)}, \mathbf{v}\right) - \left(\boldsymbol{\sigma}_h^{(n+\theta)}, \mathbf{d}(\mathbf{v})\right), \qquad \forall\, \mathbf{v} \in Z_h.\end{aligned} \tag{4.4}$$

Step 2b: Find $\boldsymbol{\sigma}_h^{(n+\tilde{\theta})} \in S_h$ such that

$$\begin{aligned}\frac{\lambda}{(1-2\theta)\Delta t}\left(\boldsymbol{\sigma}_h^{(n+\tilde{\theta})}, \boldsymbol{\tau}\right) + (1-\omega)\left(\boldsymbol{\sigma}_h^{(n+\tilde{\theta})}, \boldsymbol{\tau}_\delta^{(n+\tilde{\theta})}\right) + \lambda\left(\boldsymbol{u}_h^{(n+\tilde{\theta})} \cdot \nabla\boldsymbol{\sigma}_h^{(n+\tilde{\theta})}, \boldsymbol{\tau}_\delta^{(n+\tilde{\theta})}\right) \\ + \lambda\left(g_a(\boldsymbol{\sigma}_h^{(n+\tilde{\theta})}, \nabla\boldsymbol{u}_h^{(n+\tilde{\theta})}), \boldsymbol{\tau}_\delta^{(n+\tilde{\theta})}\right) - 2\alpha\left(\mathbf{d}(\boldsymbol{u}_h^{(n+\tilde{\theta})}), \boldsymbol{\tau}_\delta^{(n+\tilde{\theta})}\right) \\ = \frac{\lambda}{(1-2\theta)\Delta t}\left(\boldsymbol{\sigma}_h^{(n+\theta)}, \boldsymbol{\tau}\right) - \omega\left(\boldsymbol{\sigma}_h^{(n+\theta)}, \boldsymbol{\tau}_\delta^{(n+\tilde{\theta})}\right), \qquad \forall\, \boldsymbol{\tau} \in S_h.\end{aligned} \tag{4.5}$$

Step 3a: Find $\boldsymbol{\sigma}_h^{(n+1)} \in S_h$ such that

$$\begin{aligned}\frac{\lambda}{\theta\Delta t}\left(\boldsymbol{\sigma}_h^{(n+1)}, \boldsymbol{\tau}\right) + \omega\left(\boldsymbol{\sigma}_h^{(n+1)}, \boldsymbol{\tau}_\delta^{(n+\tilde{\theta})}\right) = \frac{\lambda}{\theta\Delta t}\left(\boldsymbol{\sigma}_h^{(n+\tilde{\theta})}, \boldsymbol{\tau}\right) - (1-\omega)\left(\boldsymbol{\sigma}_h^{(n+\tilde{\theta})}, \boldsymbol{\tau}_\delta^{(n+\tilde{\theta})}\right) \\ - \lambda\left(\boldsymbol{u}_h^{(n+\tilde{\theta})} \cdot \nabla\boldsymbol{\sigma}_h^{(n+\tilde{\theta})}, -\boldsymbol{\tau}_\delta^{(n+\tilde{\theta})}\right)\lambda\left(g_a(\boldsymbol{\sigma}_h^{(n+\tilde{\theta})}, \nabla - \boldsymbol{u}_h^{(n+\tilde{\theta})}), \boldsymbol{\tau}_\delta^{(n+\tilde{\theta})}\right) \\ + 2\alpha\left(-\mathbf{d}(\boldsymbol{u}_h^{(n+\tilde{\theta})}), \boldsymbol{\tau}_\delta^{(n+\tilde{\theta})}\right), \qquad \forall\, \boldsymbol{\tau} - \in S_h.\end{aligned} \tag{4.6}$$

Step 3b: Find $\boldsymbol{u}_h^{(n+1)} \in Z_h$ such that

$$\frac{Re}{\theta\Delta t}\left(\boldsymbol{u}_h^{(n+1)}, \mathbf{v}\right) + 2(1-\alpha)\left(\mathbf{d}(\boldsymbol{u}_h^{(n+1)}), \mathbf{d}(\mathbf{v})\right) = \frac{Re}{\theta\Delta t}\left(\boldsymbol{u}_h^{(n+\tilde{\theta})}, \mathbf{v}\right) + \left(\mathbf{f}^{(n+1)}, \mathbf{v}\right) - \left(\boldsymbol{\sigma}_h^{(n+1)}, \mathbf{d}(\mathbf{v})\right), \qquad \forall\, \mathbf{v} \in Z_h. \quad (4.7)$$

4.2 Existence and Uniqueness

Before error estimates are presented the computability of the θ-method is shown. This is accomplished by proving that the associated coefficient matrices used in each step of the algorithm are invertible.

The following induction hypothesis is used: There exists a constant K such that for $n = 1, \ldots, N$

$$\left\|\boldsymbol{u}_h^{(n)}\right\|_\infty, \left\|\boldsymbol{u}_h^{(n+\tilde{\theta})}\right\|_\infty \leq K. \quad \text{(IH1)}$$

The justification of (IH1) is established below.

Lemma 1 (Step 1a) *Assume (IH1) is true. For $\delta \leq Ch$ and Δt sufficiently small there exists a unique solution $\boldsymbol{\sigma}_h^{(n+\theta)} \in S_h$ satisfying (4.2).*

Proof: Equation (4.2) can be equivalently written as

$$\mathcal{A}_1\left(\boldsymbol{\sigma}_h^{(n+\theta)}, \boldsymbol{\tau}\right) = \frac{\lambda}{\theta\Delta t}\left(\boldsymbol{\sigma}_h^{(n)}, \boldsymbol{\tau}\right) - \left((1-\omega)\boldsymbol{\sigma}_h^{(n)}, \boldsymbol{\tau}_\delta^{(n)}\right) - \lambda\left(\left(\boldsymbol{u}_h^{(n)} \cdot \nabla\boldsymbol{\sigma}_h^{(n)} + g_a(\boldsymbol{\sigma}_h^n, \nabla\boldsymbol{u}_h^{(n)})\right), \boldsymbol{\tau}_\delta^{(n)}\right) + 2\alpha\left(\mathbf{d}(\boldsymbol{u}_h^{(n)}), \boldsymbol{\tau}_\delta^{(n)}\right), \quad \forall\, \boldsymbol{\tau} \in S_h, \quad (4.8)$$

where

$$\mathcal{A}_1\left(\boldsymbol{\sigma}_h^{(n+\theta)}, \boldsymbol{\tau}\right) := \frac{\lambda}{\theta\Delta t}\left(\boldsymbol{\sigma}_h^{(n+\theta)}, \boldsymbol{\tau}\right) + \omega\left(\boldsymbol{\sigma}_h^{(n+\theta)}, \boldsymbol{\tau}_\delta^{(n)}\right).$$

Here (4.8) represents a square linear system of equations $A\mathbf{x} = \mathbf{b}$. With the choice $\boldsymbol{\tau} = \boldsymbol{\sigma}_h^{(n+\theta)}$, examining the individual terms in $\mathcal{A}_1$ we see that

$$\begin{aligned}
\frac{\lambda}{\theta\Delta t}\left(\boldsymbol{\sigma}_h^{(n+\theta)}, \boldsymbol{\sigma}_h^{(n+\theta)}\right) &= \frac{\lambda}{\theta\Delta t}\left\|\boldsymbol{\sigma}_h^{(n+\theta)}\right\|^2, \\
\omega\left(\boldsymbol{\sigma}_h^{(n+\theta)}, \boldsymbol{\sigma}_h^{(n+\theta)}\right) &= \omega\left\|\boldsymbol{\sigma}_h^{(n+\theta)}\right\|^2,
\end{aligned}$$

and

$$\begin{aligned}
\omega\delta\left(\boldsymbol{\sigma}_h^{(n+\theta)}, \boldsymbol{u}_h^{(n)} \cdot \nabla\boldsymbol{\sigma}_h^{(n+\theta)}\right) &= \frac{\omega\delta}{2}\left(\boldsymbol{u}_h^{(n)}, \nabla\left(\boldsymbol{\sigma}_h^{(n+\theta)}, \boldsymbol{\sigma}_h^{(n+\theta)}\right)\right) \\
&\leq \frac{\omega\delta}{2}\left\|\boldsymbol{u}_h^{(n)}\right\|_\infty Ch^{-1}\left\|\boldsymbol{\sigma}_h^{(n+\theta)}\right\|^2 \\
&\leq \frac{\omega\delta K C h^{-1}}{2}\left\|\boldsymbol{\sigma}_h^{(n+\theta)}\right\|^2.
\end{aligned}$$

Provided $\delta \le Ch$, and $\Delta t \le (2\lambda)/(\theta\omega KC)$ then $\mathcal{A}_1\left(\boldsymbol{\sigma}_h^{(n+\theta)}, \boldsymbol{\sigma}_h^{(n+\theta)}\right) > 0$, and thus the $ker\,(\mathcal{A}_1) = \{\mathbf{0}\}$. It then follows that (4.2) has a unique solution.

■

Lemma 2 (Step 1b) *There exists a unique solution* $\boldsymbol{u}_h^{(n+\theta)} \in Z_h$ *satisfying (4.3).*

Proof: Equation (4.3) can be equivalently written as

$$\mathcal{A}_2\left(\boldsymbol{u}_h^{(n+\theta)}, \mathbf{v}\right) = \frac{Re}{\theta\Delta t}\left(\boldsymbol{u}_h^{(n)}, \mathbf{v}\right) + \left(\mathbf{f}^{(n+\theta)}, \mathbf{v}\right) - \left(\boldsymbol{\sigma}_h^{(n+\theta)}, \mathbf{d}(\mathbf{v})\right), \quad \forall\, \mathbf{v} \in Z_h,$$

where

$$\mathcal{A}_2\left(\boldsymbol{u}_h^{(n+\theta)}, \mathbf{v}\right) := \frac{Re}{\theta\Delta t}\left(\boldsymbol{u}_h^{(n+\theta)}, \mathbf{v}\right) + 2(1-\alpha)\left(\mathbf{d}(\boldsymbol{u}_h^{(n+\theta)}), \mathbf{d}(\mathbf{v})\right).$$

Note that choosing $\mathbf{v} = \boldsymbol{u}_h^{(n+\theta)}$

$$\mathcal{A}_2\left(\boldsymbol{u}_h^{(n+\theta)}, \boldsymbol{u}_h^{(n+\theta)}\right) = \frac{Re}{\theta\Delta t}\left(\boldsymbol{u}_h^{(n+\theta)}, \boldsymbol{u}_h^{(n+\theta)}\right) + 2(1-\alpha)\left(\mathbf{d}(\boldsymbol{u}_h^{(n+\theta)}), \mathbf{d}(\boldsymbol{u}_h^{(n+\theta)})\right) > 0.$$

and existence and uniqueness of a solution to (4.3) has been shown.

■

Lemma 3 (Step 2a) *There exists a unique solution* $\boldsymbol{u}_h^{(n+\tilde{\theta})} \in Z_h$ *satisfying (4.4).*

Proof: First write equation (4.4) as

$$\begin{aligned}\mathcal{A}_3\left(\boldsymbol{u}_h^{(n+\tilde{\theta})}, \mathbf{v}\right) \;&=\; \frac{Re}{(1-2\theta)\Delta t}\left(\boldsymbol{u}_h^{(n+\theta)}, \mathbf{v}\right) - 2(1-\alpha)\left(\mathbf{d}(\boldsymbol{u}_h^{(n+\theta)}), \mathbf{d}(\mathbf{v})\right)\\ &\quad + \left(\mathbf{f}^{(n+\theta)}, \mathbf{v}\right) - \left(\boldsymbol{\sigma}_h^{(n+\theta)}, \mathbf{d}(\mathbf{v})\right),\end{aligned}$$

where

$$\mathcal{A}_3\left(\boldsymbol{u}_h^{(n+\tilde{\theta})}, \mathbf{v}\right) := \frac{Re}{(1-2\theta)\Delta t}\left(\boldsymbol{u}_h^{(n+\tilde{\theta})}, \mathbf{v}\right).$$

For the choice of $\mathbf{v} = \boldsymbol{u}^{(n+\tilde{\theta})}$, the system $\mathcal{A}_3\left(\boldsymbol{u}_h^{(n+\tilde{\theta})}, \boldsymbol{u}_h^{(n+\tilde{\theta})}\right) > 0$, and the proof is complete.

■

Lemma 4 (Step 2b) *Assume (IH1) is true. For* $\delta \le Ch$ *and* Δt *sufficiently small there exists a unique solution* $\boldsymbol{\sigma}_h^{(n+\tilde{\theta})} \in S_h$ *satisfying (4.5).*

Proof: Write (4.5) as

$$\mathcal{A}_4\left(\boldsymbol{\sigma}_h^{(n+\tilde{\theta})}, \boldsymbol{\tau}\right) = \frac{\lambda}{(1-2\theta)\Delta t}\left(\boldsymbol{\sigma}_h^{(n+\theta)}, \boldsymbol{\tau}\right) - \omega\left(\boldsymbol{\sigma}_h^{(n+\theta)}, \boldsymbol{\tau}_\delta^{(n+\tilde{\theta})}\right) + 2\alpha\left(\mathbf{d}(\boldsymbol{u}_h^{(n+\tilde{\theta})}), \boldsymbol{\tau}_\delta^{(n+\tilde{\theta})}\right),$$

with

$$\begin{aligned}\mathcal{A}_4\left(\boldsymbol{\sigma}_h^{(n+\tilde{\theta})}, \boldsymbol{\tau}\right) := \;& \frac{\lambda}{(1-2\theta)\Delta t}\left(\boldsymbol{\sigma}_h^{(n+\tilde{\theta})}, \boldsymbol{\tau}\right) + (1-\omega)\left(\boldsymbol{\sigma}_h^{(n+\tilde{\theta})}, \boldsymbol{\tau}_\delta^{(n+\tilde{\theta})}\right)\\ &+ \lambda\left(\boldsymbol{u}_h^{(n+\tilde{\theta})} \cdot \nabla\boldsymbol{\sigma}_h^{(n+\tilde{\theta})}, \boldsymbol{\tau}_\delta^{(n+\tilde{\theta})}\right) + \lambda\left(g_a(\boldsymbol{\sigma}_h^{(n+\tilde{\theta})}, \nabla\boldsymbol{u}_h^{(n+\tilde{\theta})}), \boldsymbol{\tau}_\delta^{(n+\tilde{\theta})}\right).\end{aligned}$$

Estimating the terms in $\mathcal{A}_4\left(\boldsymbol{\sigma}_h^{(n+\tilde{\theta})},\boldsymbol{\sigma}_h^{(n+\tilde{\theta})}\right)$ yields

$$\frac{\lambda}{(1-2\theta)\Delta t}\left(\boldsymbol{\sigma}_h^{(n+\tilde{\theta})},\boldsymbol{\sigma}_h^{(n+\tilde{\theta})}\right)=\frac{\lambda}{(1-2\theta)\Delta t}\left\|\boldsymbol{\sigma}_h^{(n+\tilde{\theta})}\right\|^2,$$

$$(1-\omega)\left(\boldsymbol{\sigma}_h^{(n+\tilde{\theta})},\boldsymbol{\sigma}_h^{(n+\tilde{\theta})}\right)=(1-\omega)\left\|\boldsymbol{\sigma}_h^{(n+\tilde{\theta})}\right\|^2,$$

$$(1-\omega)\left(\boldsymbol{\sigma}_h^{(n+\tilde{\theta})},\delta\boldsymbol{u}_h^{(n+\tilde{\theta})}\cdot\nabla\boldsymbol{\sigma}_h^{(n+\tilde{\theta})}\right)\leq\epsilon_0\delta\left\|\boldsymbol{u}_h^{(n+\tilde{\theta})}\cdot\nabla\boldsymbol{\sigma}_h^{(n+\tilde{\theta})}\right\|^2+\frac{(1-\omega)^2\delta}{4\epsilon_0}\left\|\boldsymbol{\sigma}_h^{(n+\tilde{\theta})}\right\|^2,$$

$$\begin{aligned}\lambda\left(\boldsymbol{u}_h^{(n+\tilde{\theta})}\cdot\nabla\boldsymbol{\sigma}_h^{(n+\tilde{\theta})},\boldsymbol{\sigma}_h^{(n+\tilde{\theta})}\right)&\leq\frac{\lambda\left\|\boldsymbol{u}_h^{(n+\tilde{\theta})}\right\|_\infty Ch^{-1}}{2}\left\|\boldsymbol{\sigma}_h^{(n+\tilde{\theta})}\right\|^2\\&\leq\frac{\lambda KCh^{-1}}{2}\left\|\boldsymbol{\sigma}_h^{(n+\tilde{\theta})}\right\|^2,\end{aligned}$$

$$\lambda\left(\boldsymbol{u}_h^{(n+\tilde{\theta})}\cdot\nabla\boldsymbol{\sigma}_h^{(n+\tilde{\theta})},\delta\boldsymbol{u}_h^{(n+\tilde{\theta})}\cdot\nabla\boldsymbol{\sigma}_h^{(n+\tilde{\theta})}\right)=\lambda\delta\left\|\boldsymbol{u}_h^{(n+\tilde{\theta})}\cdot\nabla\boldsymbol{\sigma}_h^{(n+\tilde{\theta})}\right\|^2,$$

$$\begin{aligned}\lambda\left(g_a(\boldsymbol{\sigma}_h^{(n+\tilde{\theta})},\nabla\boldsymbol{u}_h^{(n+\tilde{\theta})}),\boldsymbol{\sigma}_h^{(n+\tilde{\theta})}\right)&\leq 4\lambda\left\|\boldsymbol{\sigma}_h^{(n+\tilde{\theta})}\nabla\boldsymbol{u}_h^{(n+\tilde{\theta})}\right\|\left\|\boldsymbol{\sigma}_h^{(n+\tilde{\theta})}\right\|\\&\leq 4\acute{d}^{1/2}\lambda\left\|\nabla\boldsymbol{u}_h^{(n+\tilde{\theta})}\right\|_\infty\left\|\boldsymbol{\sigma}_h^{(n+\tilde{\theta})}\right\|^2\\&\leq 4\acute{d}^{1/2}\lambda Ch^{-1}\left\|\boldsymbol{u}_h^{(n+\tilde{\theta})}\right\|_\infty\left\|\boldsymbol{\sigma}_h^{(n+\tilde{\theta})}\right\|^2\\&\leq 4\acute{d}^{1/2}\lambda Ch^{-1}K\left\|\boldsymbol{\sigma}_h^{(n+\tilde{\theta})}\right\|^2,\end{aligned}$$

$$\begin{aligned}\left(\lambda g_a(\boldsymbol{\sigma}_h^{(n+\tilde{\theta})},\nabla\boldsymbol{u}_h^{(n+\tilde{\theta})}),\delta\boldsymbol{u}_h^{(n+\tilde{\theta})}\cdot\nabla\boldsymbol{\sigma}_h^{(n+\tilde{\theta})}\right)&\leq 4\lambda\left\|\boldsymbol{\sigma}_h^{(n+\tilde{\theta})}\nabla\boldsymbol{u}_h^{(n+\tilde{\theta})}\right\|\left\|\delta\boldsymbol{u}_h^{(n+\tilde{\theta})}\cdot\nabla\boldsymbol{\sigma}_h^{(n+\tilde{\theta})}\right\|\\&\leq 4\acute{d}^{1/2}\lambda\left\|\nabla\boldsymbol{u}_h^{(n+\tilde{\theta})}\right\|_\infty\left\|\boldsymbol{\sigma}_h^{(n+\tilde{\theta})}\right\|\left\|\delta\boldsymbol{u}_h^{(n+\tilde{\theta})}\cdot\nabla\boldsymbol{\sigma}_h^{(n+\tilde{\theta})}\right\|\\&\leq\frac{4\acute{d}\lambda C^2h^{-2}K^2\delta}{\epsilon_1}\left\|\boldsymbol{\sigma}_h^{(n+\tilde{\theta})}\right\|^2+\lambda\epsilon_1\delta\left\|\boldsymbol{u}_h^{(n+\tilde{\theta})}\cdot\nabla\boldsymbol{\sigma}_h^{(n+\tilde{\theta})}\right\|^2.\end{aligned}$$

Thus,

$$\begin{aligned}\mathcal{A}_4(\boldsymbol{\sigma}_h^{(n+\tilde{\theta})},\boldsymbol{\sigma}_h^{(n+\tilde{\theta})})\quad\geq\quad&\left(\frac{\lambda}{(1-2\theta)\Delta t}+(1-\omega)-\frac{(1-\omega)^2\delta}{4\epsilon_0}\right.\\&\left.-\lambda KCh^{-1}\left(\frac{1}{2}+4\acute{d}^{1/2}+\frac{4\acute{d}KCh^{-1}\delta}{\epsilon_1}\right)\right)\left\|\boldsymbol{\sigma}_h^{(n+\tilde{\theta})}\right\|^2\\&+\delta\left(\lambda-\epsilon_0-\lambda\epsilon_1\right)\left\|\boldsymbol{u}_h^{(n+\tilde{\theta})}\cdot\nabla\boldsymbol{\sigma}_h^{(n+\tilde{\theta})}\right\|^2.\end{aligned}$$

Choosing $\epsilon_0 = \frac{\lambda}{3}$, $\epsilon_1 = \frac{1}{3}$, $\delta \le \mathcal{C}h^{-1}$, and $\Delta t \le \mathcal{C}h^{-1}$ establishes $\mathcal{A}_4(\boldsymbol{\sigma}_h^{(n+\tilde{\theta})}, \boldsymbol{\sigma}_h^{(n+\tilde{\theta})}) > 0$. Hence, a unique solution exists for (4.2).

■

The unique solvability of (4.6) and (4.7) of the algorithm follows exactly as (4.2) and (4.3).

4.3 Error Estimates

In this section supporting analysis for the θ-method described in Section 2 is given. The θ-method decouples the stress updates from the velocity-pressure updates. Though the modeling system is nonlinear, the updates for the stress and velocity-pressure only require linear systems of equations to be solved. Motivated by this decoupling (as a first step toward an analysis of the fully discretized system) we investigate separately the stress and velocity-pressure approximations. First a θ-method for the constitutive equation given by (4.2), (4.5), and (4.6) is investigated assuming the velocity and pressure are known. Then a θ-method for the Stokes-like problem given by (4.3), (4.4), and (4.7) is analyzed assuming the stress is known. A priori error estimates for each scheme are given in Theorems 4.1 and 4.2, and a discussion of the proofs is given below. (Detailed proofs are given in [8].)

It is convenient to define the following notation:

$$\begin{aligned} \tilde{\boldsymbol{u}}_h &:= \text{discrete approximation using true } \boldsymbol{\sigma}, \\ \tilde{\boldsymbol{\sigma}}_h &:= \text{discrete approximation using true } \boldsymbol{u}, \text{ and } p. \end{aligned}$$

Theorem 4.1 (Assuming u and p are known) *For sufficiently smooth solutions $\boldsymbol{\sigma}$, $\boldsymbol{u}$, p such that*

$$\|\boldsymbol{u}\|_\infty, \|\boldsymbol{u}_t\|_\infty, \|\boldsymbol{u}_{tt}\|_\infty, \|\nabla\boldsymbol{u}\|_\infty, \|(\nabla\boldsymbol{u})_t\|_\infty, \ \textit{and} \ \ \|(\nabla\boldsymbol{u})_{tt}\|_\infty \le M, \quad \forall\, t \in [0,T],$$

$\Delta t \le Ch^2$, the fractional step θ-method approximation, $\tilde{\boldsymbol{\sigma}}_h$ given by Step 1a, Step 2b, and Step 3a converges to $\boldsymbol{\sigma}$ on the interval $(0,T]$ as $\Delta t, h \to 0$, and satisfies the error estimates:

$$|||\boldsymbol{\sigma} - \tilde{\boldsymbol{\sigma}}_h|||_{\infty,0} \le F_{\boldsymbol{\sigma}}(\Delta t, h, \delta), \tag{4.9}$$

$$|||\boldsymbol{\sigma} - \tilde{\boldsymbol{\sigma}}_h|||_{0,0} \le F_{\boldsymbol{\sigma}}(\Delta t, h, \delta), \tag{4.10}$$

and

$$|||\boldsymbol{u}\cdot\nabla(\boldsymbol{\sigma} - \tilde{\boldsymbol{\sigma}}_h)|||_{\tilde{\theta}} := \left(\sum_{n=1}^{N} \Delta t \left\| \boldsymbol{u}^{(n+\tilde{\theta})} \cdot \nabla\left(\boldsymbol{\sigma}^{(n+\tilde{\theta})} - \tilde{\boldsymbol{\sigma}}_h^{(n+\tilde{\theta})}\right)\right\|^2\right)^{\frac{1}{2}} \le F_{\boldsymbol{\sigma}}(\Delta t, h, \delta), \tag{4.11}$$

where

$$\begin{aligned} F_{\boldsymbol{\sigma}}(\Delta t, h, \delta) \ := \ & C(\Delta t)^2\Big(\|\boldsymbol{\sigma}_{ttt}\|_{0,0} + \|\boldsymbol{\sigma}_{tt}\|_{0,1} + \|\boldsymbol{\sigma}_t\|_{0,1} + \|\boldsymbol{\sigma}\|_{0,1} \\ & \qquad + \ \|\boldsymbol{\sigma}_{tt}\|_{0,0} + \|\boldsymbol{\sigma}_t\|_{0,0} + \|\boldsymbol{\sigma}\|_{0,0} + C_T\Big) \\ & + C(\Delta t)\delta\left(\|\boldsymbol{\sigma}\|_{0,1} + \|\boldsymbol{\sigma}_t\|_{0,1} + \|\boldsymbol{\sigma}\|_{0,0} + \|\boldsymbol{\sigma}_t\|_{0,0} + C_T\right) \\ & + C\left(h^{m+1} + h^m + \delta h^m\right)|||\boldsymbol{\sigma}|||_{0,m+1} \\ & + Ch^{m+1}\|\boldsymbol{\sigma}_t\|_{0,m+1} + \ C\delta\,|||\boldsymbol{\sigma}_t|||_{0,0} + Ch^{m+1}\,|||\boldsymbol{\sigma}|||_{\infty,0}\,. \end{aligned} \tag{4.12}$$

Theorem 4.2 (Assuming $\boldsymbol{\sigma}$ is known) *For a sufficiently smooth solutions $\boldsymbol{u}$, $\boldsymbol{\sigma}$, p such that $\|\boldsymbol{\sigma}\|_\infty \le M,\ \ \forall\, t \in [0,T]$, and $\Delta t \le Ch^2$, the fractional step θ-method approximation, $\tilde{\boldsymbol{u}}_h$ given by Step 1b, Step 2a, and Step 3b converges to $\boldsymbol{u}$ on the interval $(0,T]$ as $\Delta t, h \to 0$, and satisfies the error estimates:*

$$|||\boldsymbol{u} - \tilde{\boldsymbol{u}}_h|||_{\infty,0} \le F_{\boldsymbol{u}}(\Delta t, h, \delta), \tag{4.13}$$

and

$$|||\boldsymbol{u} - \tilde{\boldsymbol{u}}_h|||_{0,1} \le F_{\boldsymbol{u}}(\Delta t, h, \delta), \tag{4.14}$$

where

$$\begin{aligned} F_{\boldsymbol{u}}(\Delta t, h, \delta) \;\; &:= \;\; Ch^{k+1}\,\|\boldsymbol{u}_t\|_{0,k+1} + Ch^k\,|||\boldsymbol{u}|||_{0,k+1} + Ch^{q+1}\,|||p|||_{0,q+1} \\ &\quad + C(\Delta t)^2\,\|\boldsymbol{u}_{ttt}\|_{0,0} + C(\Delta t)^2\,\|\boldsymbol{u}_{tt}\|_{0,1} + C(\Delta t)^2\,\|\mathbf{f}_{tt}\|_{0,0} \\ &\quad + C(\Delta t)^2 C_T + Ch^k\,|||\boldsymbol{u}|||_{\infty,k+1}\,. \end{aligned} \tag{4.15}$$

Outline of the proof. In [6], and [7] the analysis for a fractional step θ-method for the convection diffusion equation was presented. The proof of Theorems 4.1 and 4.2 are done in an analogous manner to the proof presented in [7]. Here we present an outline of the proof for Theorem 4.1, and note that the proof of Theorem 4.2 is accomplished in a similar manner.

Step 1. When obtaining a priori error estimates for the time dependent approximation schemes it is useful to examine a *unit stride*, i.e. the terms analyzed are distance Δt apart. For the θ-method this is accomplished by considering linear combinations of the approximation methods steps. In order to obtain *unit strides* from $\tilde{\boldsymbol{\sigma}}_h^{(n)}$ to $\tilde{\boldsymbol{\sigma}}_h^{(n+1)}$, $\tilde{\boldsymbol{\sigma}}_h^{(n-\theta)}$ to $\tilde{\boldsymbol{\sigma}}_h^{(n+\tilde{\theta})}$, and $\tilde{\boldsymbol{\sigma}}_h^{(n+\theta-1)}$ to $\tilde{\boldsymbol{\sigma}}_h^{(n+\theta)}$ the following linear combinations are formed:

$$\theta\Delta t(4.2) + (1-2\theta)\,\Delta t(4.5) + \theta\Delta t(4.6), \tag{4.16}$$

$$\theta\Delta t(4.2) + (1-2\theta)\,\Delta t(4.5) + \theta\Delta t\,((4.6) \text{ with } n \to n-1)\,, \tag{4.17}$$

$$\theta\Delta t(4.2) + (1-2\theta)\,\Delta t\,((4.5) \text{ with } n \to n-1) + \theta\Delta t\,((4.6) \text{ with } n \to n-1)\,. \tag{4.18}$$

Step 2. Evaluate (3.7) at the midpoint of each *unit stride* and subtract equations (4.16)-(4.18). Rearrange terms to obtain the equations:

$$\begin{aligned} &\left(\left(\boldsymbol{\sigma}^{(n+1)} - \tilde{\boldsymbol{\sigma}}_h^{(n+1)}\right) - \left(\boldsymbol{\sigma}^{(n)} - \tilde{\boldsymbol{\sigma}}_h^{(n)}\right), \boldsymbol{\tau}\right) + \Delta t \mathcal{B}_{1_{pos}}\left(\left(\boldsymbol{\sigma}^{(n+1)} - \tilde{\boldsymbol{\sigma}}_h^{(n+1)}\right), \boldsymbol{\tau}\right) \\ &\qquad = \Delta t \mathcal{B}_{1_{rem}}\left(\Delta t, \boldsymbol{\sigma}, \boldsymbol{u}, \tilde{\boldsymbol{\sigma}}_h^{(n+1)}, \tilde{\boldsymbol{\sigma}}_h^{(n+\tilde{\theta})}, \tilde{\boldsymbol{\sigma}}_h^{(n+\theta)}, \tilde{\boldsymbol{\sigma}}_h^{(n)}, \boldsymbol{\tau}\right), \end{aligned} \tag{4.19}$$

$$\begin{aligned} &\left(\left(\boldsymbol{\sigma}^{(n+\tilde{\theta})} - \tilde{\boldsymbol{\sigma}}_h^{(n+\tilde{\theta})}\right) - \left(\boldsymbol{\sigma}^{(n-\theta)} - \tilde{\boldsymbol{\sigma}}_h^{(n-\theta)}\right), \boldsymbol{\tau}\right) + \Delta t \mathcal{B}_{2_{pos}}\left(\left(\boldsymbol{\sigma}^{(n+\tilde{\theta})} - \tilde{\boldsymbol{\sigma}}_h^{(n+\tilde{\theta})}\right), \boldsymbol{\tau}\right) \\ &\qquad = \Delta t \mathcal{B}_{2_{rem}}\left(\Delta t, \boldsymbol{\sigma}, \boldsymbol{u}, \tilde{\boldsymbol{\sigma}}_h^{(n+\tilde{\theta})}, \tilde{\boldsymbol{\sigma}}_h^{(n+\theta)}, \tilde{\boldsymbol{\sigma}}_h^{(n-\theta)}, \tilde{\boldsymbol{\sigma}}_h^{(n)}, \boldsymbol{\tau}\right), \end{aligned} \tag{4.20}$$

$$\left(\left(\boldsymbol{\sigma}^{(n+\theta)}-\tilde{\boldsymbol{\sigma}}_h^{(n+\theta)}\right)-\left(\boldsymbol{\sigma}^{(n+\theta-1)}-\tilde{\boldsymbol{\sigma}}_h^{(n+\theta-1)}\right),\boldsymbol{\tau}\right)+\Delta t\mathcal{B}_{3_{pos}}\left(\left(\boldsymbol{\sigma}^{(n+\theta)}-\tilde{\boldsymbol{\sigma}}_h^{(n+\theta)}\right),\boldsymbol{\tau}\right)$$
$$=\Delta t\mathcal{B}_{3_{rem}}\left(\Delta t,\boldsymbol{\sigma},\boldsymbol{u},\tilde{\boldsymbol{\sigma}}_h^{(n+\theta-1)},\tilde{\boldsymbol{\sigma}}_h^{(n+\theta)},\tilde{\boldsymbol{\sigma}}_h^{(n-\theta)},\tilde{\boldsymbol{\sigma}}_h^{(n)},\boldsymbol{\tau}\right), \quad (4.21)$$

where $\mathcal{B}_{1_{pos}}$, $\mathcal{B}_{2_{pos}}$, and $\mathcal{B}_{3_{pos}}$ denote the positive part of the operators.

Step 3. Use $\boldsymbol{\sigma}^{(n)}-\tilde{\boldsymbol{\sigma}}_h^{(n)}=\tilde{\boldsymbol{\Gamma}}^{(n)}+\tilde{\boldsymbol{F}}^{(n)}$, and choose $\boldsymbol{\tau}=\tilde{\boldsymbol{F}}^{(n)}$, in (4.19) to obtain an expression of the form

$$\left\|\boldsymbol{F}^{(n+1)}\right\|^2-\left\|\boldsymbol{F}^{(n)}\right\|^2+\Delta t\mathcal{B}_{1_{pos}}\left(\tilde{\boldsymbol{F}}^{(n+1)},\tilde{\boldsymbol{F}}^{(n+1)}\right)\leq\Delta t\tilde{\mathcal{B}}_{1_{rem}}\left(\Delta t,\boldsymbol{\sigma},\boldsymbol{u},\tilde{\boldsymbol{\Gamma}},\tilde{\boldsymbol{F}}\right). \quad (4.22)$$

Assuming that $\boldsymbol{F}^{(0)}=0$, (4.22) is then summed from $n=0$ to $n=l-1$ so that the expression *telescopes* to

$$\left\|\boldsymbol{F}^l\right\|^2+\Delta t\sum_{n=0}^{l-1}\mathcal{B}_{1_{pos}}\left(\tilde{\boldsymbol{F}}^{(n+1)},\tilde{\boldsymbol{F}}^{(n+1)}\right)=\Delta t\mathcal{R}_1\left(\Delta t,\boldsymbol{\sigma},\boldsymbol{u},\tilde{\boldsymbol{\Gamma}},\tilde{\boldsymbol{F}}\right). \quad (4.23)$$

A similar approach is taken with (4.20) and (4.21) where $\boldsymbol{\tau}$ is chosen to be $\boldsymbol{F}^{(n+\tilde{\theta})}$ and $\boldsymbol{F}^{(n+\theta)}$, respectively, giving equations for $\left\|\boldsymbol{F}^{(l-\theta)}\right\|^2$, and $\left\|\boldsymbol{F}^{(l-1+\theta)}\right\|^2$. These three equations are then added together to form a single equation.

Step 4. Suitable inequalities/estimates are then applied to the terms in the equation.

Step 5. Gronwall's lemma is applied to get an estimate for $\left\|\tilde{\boldsymbol{F}}^{l-1+\theta}\right\|^2+\left\|\tilde{\boldsymbol{F}}^{l-\theta}\right\|^2+\left\|\tilde{\boldsymbol{F}}^{l}\right\|^2$, and then using the triangle inequality we obtain the error estimate for $\left\|\boldsymbol{\sigma}^{(l)}-\tilde{\boldsymbol{\sigma}}_h^{(l)}\right\|+\left\|\boldsymbol{\sigma}^{(l-\theta)}-\tilde{\boldsymbol{\sigma}}_h^{(l-\theta)}\right\|+\left\|\boldsymbol{\sigma}^{(l-1+\theta)}-\tilde{\boldsymbol{\sigma}}_h^{(l-1+\theta)}\right\|$.

■

In Section 5 the numerical results presented use continuous, piecewise linear approximations for $\boldsymbol{\sigma}$, and p, and a continuous, piecewise quadratic approximation for $\boldsymbol{u}$. With these approximations we have the following estimates:

Corollary 1 *For S_h the space of continuous, piecewise linear functions, $\Delta t\leq Ch^2$, and $\boldsymbol{\sigma},\boldsymbol{u},p$ sufficiently smooth, the approximation $\tilde{\boldsymbol{\sigma}}_h$ satisfies the error estimate:*

$$|||\boldsymbol{u}\cdot\nabla\left(\boldsymbol{\sigma}-\tilde{\boldsymbol{\sigma}}_h\right)|||_{\tilde{\theta}}\leq C\left((\Delta t)^2+\Delta t\delta+h\delta+h+\delta\right). \quad (4.24)$$

Corollary 2 *For X_h the space of continuous, piecewise quadratic functions, and Q_h the space of continuous, piecewise linear functions, $\Delta t\leq Ch^2$, and $\boldsymbol{\sigma},\boldsymbol{u},p$ sufficiently smooth, the approximation $\tilde{\boldsymbol{u}}_h$ satisfies the error estimate:*

$$|||\boldsymbol{u}-\tilde{\boldsymbol{u}}_h|||_{0,1}\leq C\left((\Delta t)^2+h^2\right). \quad (4.25)$$

Justification of (IH1) for $\tilde{\boldsymbol{u}}_h$.

Assume that (IH1) holds for $n = 1, 2, \ldots, l-1$. Then using inverse estimates, interpolation properties, and (4.15)

$$
\begin{aligned}
\left\|\boldsymbol{u}_h^l\right\|_\infty &\leq \left\|\boldsymbol{u}_h^l - \boldsymbol{u}^l\right\|_\infty + \left\|\boldsymbol{u}^l\right\|_\infty \\
&\leq \left\|\boldsymbol{E}^l\right\|_\infty + \left\|\Lambda^l\right\|_\infty + M \\
&\leq Ch^{\frac{-\acute{d}}{2}}\left\|\boldsymbol{E}^l\right\| + Ch^{\frac{-\acute{d}}{2}}\left\|\Lambda^l\right\| + M \\
&\leq C\left(h^{k-\frac{\acute{d}}{2}} + h^{q-\frac{\acute{d}}{2}+1} + (\Delta t)^2 h^{\frac{-\acute{d}}{2}} + h^{k-\frac{\acute{d}}{2}+1}\right) + M. \qquad (4.26)
\end{aligned}
$$

Setting $k \geq \frac{\acute{d}}{2}$, and $q \geq \frac{\acute{d}}{2} - 1$ and choosing h, and Δt such that

$$
h^{k-\frac{\acute{d}}{2}}, h^{q-\frac{\acute{d}}{2}+1} \leq \frac{1}{C}, \quad \text{and} \quad \Delta t^2 \leq \frac{h^{\frac{\acute{d}}{2}}}{C}, \qquad (4.27)
$$

we have

$$
\left\|\boldsymbol{u}_h^l\right\|_\infty \leq M + 4.
$$

Similarly it follows that $\left\|\boldsymbol{u}_h^{(n+\tilde{\theta})}\right\|_\infty \leq M + 4.$

■

5 Numerical Results

In this section we present numerical results for the θ-method on two test problems. The first example uses a known analytical solution to verify numerical convergence rates (Cvge. Rate) of the θ-method. In the second example, we considered a prototypal problem of viscoelastic flow, flow through a 4:1 planar contraction. In both examples finite element computations were carried out using the FreeFem++ integrated development environment [14]. Continuous piecewise quadratic elements were used for modeling the velocity, and continuous piecewise linear elements were used for the pressure and stress. The constitutive equation was stabilized using a SUPG discretization with a parameter δ.

For the (optimal) value of $\theta = 1 - \sqrt{2}/2 \approx 0.29289$ the local temporal discretization errors are $O((\Delta t)^2)$. The influence of the value for θ on the numerical approximations is illustrated in Figure 5.1. for computations performed on Example 1 (described below). All the other computations reported in this paper were obtained using $\theta = 1 - \sqrt{2}/2$. The constitutive equation splitting parameter ω was set to 1/2 in all computations.

5.1 Example 1

In order to investigate the predicted convergence rates we consider fluid flow across a unit square with a known solution.

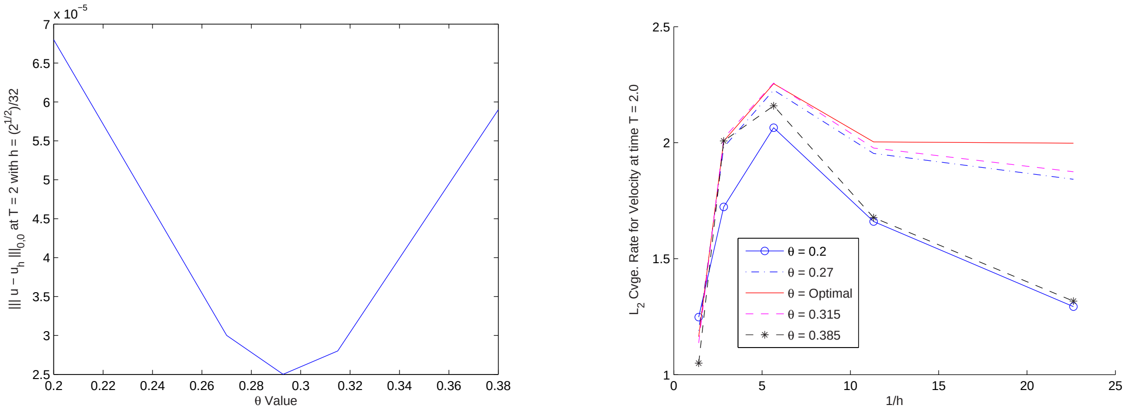

(a) Error $|||\boldsymbol{u} - \boldsymbol{u}_h|||_{0,0}$ as a function of θ.

(b) Experimental convergence rates.

Figure 5.1: Optimal θ value

Let $\Omega = (0,1) \times (0,1), Re = 1, \alpha = 1/2, \lambda = 2$, and $a = 1$. For the true solution we use

$$\boldsymbol{u} = \begin{pmatrix} e^{\left(x+y-\frac{1}{2}t\right)}(x^2 - x)(y^2 - y) \\ -e^{(x+y-t)}(x^2 - x)(y^2 - y) \end{pmatrix}, \tag{5.1}$$

$$p = \cos(2\pi x)(y^2 - y), \tag{5.2}$$

$$\boldsymbol{\sigma} = 2\alpha \mathbf{d}(\boldsymbol{u}). \tag{5.3}$$

Remark: A right-hand-side function is added to (2.1) and $\mathbf{f}$ in (2.2) is calculated using (5.1)-(5.3).

For this example three sequences of computations were performed:

(i) approximation of $\tilde{\boldsymbol{\sigma}}_h$, assuming $\boldsymbol{u}$ and p (Theorem 4.1),

(ii) approximation of $\tilde{\boldsymbol{u}}_h$ and $\tilde{p}_h$, assuming $\boldsymbol{\sigma}$ (Theorem 4.2),

(iii) approximation of $\boldsymbol{u}_h, p_h$ and $\boldsymbol{\sigma}_h$.

5.1.1 Approximating $\tilde{\boldsymbol{\sigma}}_h$ with $\boldsymbol{u}$ and p known

We first consider the approximation of the stress $\tilde{\boldsymbol{\sigma}}_h$ assuming the velocity and pressure functions are known. This is analogous to implementing Step 1a, Step 2b, and Step 3a of the θ-method. From Corollary 1 we have predicted asymptotic convergence rate

$$|||\boldsymbol{u} \cdot \nabla (\boldsymbol{\sigma} - \tilde{\boldsymbol{\sigma}}_h)|||_{\tilde{\theta}} \leq C\left((\Delta t)^2 + \Delta t \delta + h\delta + h + \delta\right),$$

which is consistent with the numerical convergence rates presented in Table 5.1. Note Table 5.1 shows the effect of the upwinding parameter δ on $|||\boldsymbol{\sigma} - \tilde{\boldsymbol{\sigma}}_h|||_{0,0}$.

For the proof of Theorem 4.1 we required the restriction $\Delta t \leq Ch^2$. The numerical computations were performed with $\Delta t \sim h$. It is an open question if the restriction $\Delta t \leq Ch^2$ is a necessary condition for (4.12).

Table 5.1: Approximation errors and experimental convergence rates at $T = 2$

$\delta \downarrow$	$(\Delta t, h) \rightarrow$	$\left(1, \frac{\sqrt{2}}{2}\right)$	$\left(\frac{1}{2}, \frac{\sqrt{2}}{4}\right)$	$\left(\frac{1}{4}, \frac{\sqrt{2}}{8}\right)$	$\left(\frac{1}{8}, \frac{\sqrt{2}}{16}\right)$	$\left(\frac{1}{16}, \frac{\sqrt{2}}{32}\right)$
0	$\|\|\|\boldsymbol{\sigma} - \tilde{\boldsymbol{\sigma}}_h\|\|\|_{0,0}$	2.1235e-1	6.6773e-2	1.9191e-2	5.0437e-3	1.2830e-3
	Cvge. Rate	-	1.7	1.8	1.9	2.0
	$\|\|\|\boldsymbol{u} \cdot \nabla(\boldsymbol{\sigma} - \tilde{\boldsymbol{\sigma}}_h)\|\|\|_{\tilde{\theta}}$	1.1544e-1	6.1759e-2	2.9979e-2	1.5185e-2	7.6944e-3
	Cvge. Rate	-	0.9	1.0	1.0	1.0
$\frac{h}{\sqrt{2}}$	$\|\|\|\boldsymbol{\sigma} - \tilde{\boldsymbol{\sigma}}_h\|\|\|_{0,0}$	2.0070e-1	8.4563e-2	3.7449e-2	1.6980e-2	8.0428e-3
	Cvge. Rate	-	1.2	1.2	1.1	1.1
	$\|\|\|\boldsymbol{u} \cdot \nabla(\boldsymbol{\sigma} - \tilde{\boldsymbol{\sigma}}_h)\|\|\|_{\tilde{\theta}}$	1.0263e-1	6.4336e-2	3.2570e-2	1.6325e-2	8.2071e-3
	Cvge. Rate	-	0.7	1.0	1.0	1.0
$\left(\frac{h}{\sqrt{2}}\right)^{\frac{3}{2}}$	$\|\|\|\boldsymbol{\sigma} - \tilde{\boldsymbol{\sigma}}_h\|\|\|_{0,0}$	2.0174e-1	7.3678e-2	2.3575e-2	6.9629e-3	2.0645e-3
	Cvge. Rate	-	1.5	1.6	1.8	1.8
	$\|\|\|\boldsymbol{u} \cdot \nabla(\boldsymbol{\sigma} - \tilde{\boldsymbol{\sigma}}_h)\|\|\|_{\tilde{\theta}}$	1.0447e-1	6.2239e-2	3.0497e-2	1.5304e-2	7.7199e-3
	Cvge. Rate	-	0.7	1.0	1.0	1.0
$\left(\frac{h}{\sqrt{2}}\right)^{2}$	$\|\|\|\boldsymbol{\sigma} - \tilde{\boldsymbol{\sigma}}_h\|\|\|_{0,0}^2$	2.0346e-1	6.9501e-2	2.0245e-2	5.3281e-3	1.3546e-3
	Cvge. Rate	-	1.5	1.8	1.9	2.0
	$\|\|\|\boldsymbol{u} \cdot \nabla(\boldsymbol{\sigma} - \tilde{\boldsymbol{\sigma}}_h)\|\|\|_{\tilde{\theta}}$	1.0664e-1	6.1737e-2	3.0104e-2	1.5203e-2	7.6968e-3
	Cvge. Rate	-	0.8	1.0	1.0	1.0

5.1.2 Approximating $\tilde{\boldsymbol{u}}_h$ and $\tilde{p}_h$ with known $\boldsymbol{\sigma}$

Numerical results for the approximation of velocity, $\tilde{\boldsymbol{u}}_h$, and pressure, $\tilde{p}_h$ for a known stress, $\boldsymbol{\sigma}$, are presented in Table 5.2. These results correspond to the analysis of step 1b, step 2a, and step 3b as stated in Theorem 4.2.

The numerical convergence rates observed are consistent with those predicted in Corollary 2 where

$$|||\boldsymbol{u} - \tilde{\boldsymbol{u}}_h|||_{0,1} \leq O\left((\Delta t)^2 + h^2\right).$$

Similar to the case in the previous subsection we make note that the proof of Theorem 4.2 required the restriction $\Delta t \leq Ch^2$. Here the numerical computations were performed with $\Delta t \sim h$.

5.1.3 Full θ-method approximation for viscoelasticity

Table 5.3 contains the results for the approximation of $\boldsymbol{u}$ and $\boldsymbol{\sigma}$ using the θ-method described in Step 1a - Step 3b. The numerical convergence rates are consistent with our expectations based on Theorems 4.1 and 4.2, i.e.

$$|||\boldsymbol{u} - \boldsymbol{u}_h|||_{0,1} + |||\boldsymbol{\sigma} - \boldsymbol{\sigma}_h|||_{0,0} + |||\boldsymbol{u} \cdot \nabla(\boldsymbol{\sigma} - \boldsymbol{\sigma}_h)|||_{\tilde{\theta}} \sim O\left((\Delta t)^2 + (\Delta t)\,\delta + \delta + h\right).$$

Table 5.2: Approximation errors and experimental convergence rates at $T = 2$

$(\Delta t, h) \rightarrow$	$\left(\frac{1}{2}, \frac{\sqrt{2}}{4}\right)$	$\left(\frac{1}{4}, \frac{\sqrt{2}}{8}\right)$	$\left(\frac{1}{8}, \frac{\sqrt{2}}{16}\right)$	$\left(\frac{1}{16}, \frac{\sqrt{2}}{32}\right)$	$\left(\frac{1}{32}, \frac{\sqrt{2}}{64}\right)$	$\left(\frac{1}{64}, \frac{\sqrt{2}}{128}\right)$
$\lvert\lvert\lvert \boldsymbol{u} - \tilde{\boldsymbol{u}}_h \rvert\rvert\rvert_{0,1}$	4.4196e-2	1.1485e-2	2.9707e-3	7.5759e-4	1.9142e-4	4.8129e-5
Cvge. Rate	-	1.9	2.0	2.0	2.0	2.0
$\lvert\lvert\lvert \boldsymbol{u} - \tilde{\boldsymbol{u}}_h \rvert\rvert\rvert_{\infty,0}$	1.4734e-3	1.7996e-4	2.5014e-5	4.1759e-6	8.5692e-7	2.1636e-7
Cvge. Rate	-	3.0	2.8	2.6	2.3	2.0
$\lvert\lvert\lvert p - \tilde{p}_h \rvert\rvert\rvert_{0,0}$	1.0859e-1	6.6842e-3	1.5033e-3	3.9097e-4	1.2086e-4	4.7884e-5
Cvge. Rate	-	4.0	2.2	1.9	1.7	1.3
$\lvert\lvert\lvert p - \tilde{p}_h \rvert\rvert\rvert_{\infty,0}$	8.4003e-2	4.9703e-3	1.1343e-3	3.2878e-4	1.2797e-4	6.0659e-5
Cvge. Rate	-	4.1	2.1	1.8	1.4	1.1

Table 5.3: Approximation errors and experimental convergence rates at $T = 2$

$\delta \downarrow$	$(\Delta t, h) \rightarrow$	$\left(\frac{1}{2}, \frac{\sqrt{2}}{4}\right)$	$\left(\frac{1}{4}, \frac{\sqrt{2}}{8}\right)$	$\left(\frac{1}{8}, \frac{\sqrt{2}}{16}\right)$	$\left(\frac{1}{16}, \frac{\sqrt{2}}{32}\right)$	$\left(\frac{1}{32}, \frac{\sqrt{2}}{64}\right)$
0	$\lvert\lvert\lvert \boldsymbol{u} - \boldsymbol{u}_h \rvert\rvert\rvert_{0,1}$	4.7608e-2	1.2323e-2	3.2034e-3	8.3187e-4	2.1793e-4
	Cvge. Rate	-	1.9	1.9	1.9	1.9
	$\lvert\lvert\lvert \boldsymbol{\sigma} - \boldsymbol{\sigma}_h \rvert\rvert\rvert_{0,0}$	6.5569e-2	1.9248e-2	5.0845e-3	1.3000e-3	3.2981e-4
	Cvge. Rate	-	1.8	1.9	2.0	2.0
	$\lvert\lvert\lvert \boldsymbol{u} \cdot \nabla(\boldsymbol{\sigma} - \boldsymbol{\sigma}_h) \rvert\rvert\rvert_{\tilde{\theta}}$	6.1217e-2	2.9982e-2	1.5191e-2	7.6984e-3	3.8800e-3
	Cvge. Rate	-	1.0	1.0	1.0	1.0
$\frac{h}{\sqrt{2}}$	$\lvert\lvert\lvert \boldsymbol{u} - \boldsymbol{u}_h \rvert\rvert\rvert_{0,1}$	5.0150e-2	1.6193e-2	6.4636e-3	2.9147e-3	1.3989e-3
	Cvge. Rate	-	1.6	1.3	1.1	1.1
	$\lvert\lvert\lvert \boldsymbol{\sigma} - \boldsymbol{\sigma}_h \rvert\rvert\rvert_{0,0}$	8.1922e-2	3.5905e-2	1.5791e-2	7.3743e-3	3.5789e-3
	Cvge. Rate	-	1.2	1.2	1.1	1.0
	$\lvert\lvert\lvert \boldsymbol{u} \cdot \nabla(\boldsymbol{\sigma} - \boldsymbol{\sigma}_h) \rvert\rvert\rvert_{\tilde{\theta}}$	6.4087e-2	3.2589e-2	1.6309e-2	8.2007e-3	4.1180e-4
	Cvge. Rate	-	1.0	1.0	1.0	1.0
$\left(\frac{h}{\sqrt{2}}\right)^{\frac{3}{2}}$	$\lvert\lvert\lvert \boldsymbol{u} - \boldsymbol{u}_h \rvert\rvert\rvert_{0,1}$	4.8620e-2	1.3135e-2	3.6334e-3	1.0192e-3	2.9513e-4
	Cvge. Rate	-	1.9	1.9	1.8	1.8
	$\lvert\lvert\lvert \boldsymbol{\sigma} - \boldsymbol{\sigma}_h \rvert\rvert\rvert_{0,0}$	7.1941e-2	2.3392e-2	6.8309e-3	1.9976e-3	6.0598e-4
	Cvge. Rate	-	1.6	1.8	1.8	1.7
	$\lvert\lvert\lvert \boldsymbol{u} \cdot \nabla(\boldsymbol{\sigma} - \boldsymbol{\sigma}_h) \rvert\rvert\rvert_{\tilde{\theta}}$	6.1860e-2	3.0510e-2	1.5305e-2	7.7221e-3	3.8851e-3
	Cvge. Rate	-	1.0	1.0	1.0	1.0
$\left(\frac{h}{\sqrt{2}}\right)^{2}$	$\lvert\lvert\lvert \boldsymbol{u} - \boldsymbol{u}_h \rvert\rvert\rvert_{0,1}$	4.8022e-2	1.2507e-2	3.2644e-3	8.4818e-4	2.2193e-4
	Cvge. Rate	-	1.9	1.9	1.9	1.9
	$\lvert\lvert\lvert \boldsymbol{\sigma} - \boldsymbol{\sigma}_h \rvert\rvert\rvert_{0,0}$	6.8104e-2	2.0308e-2	5.3614e-3	1.3680e-3	3.4645e-4
	Cvge. Rate	-	1.7	1.9	2.0	2.0
	$\lvert\lvert\lvert \boldsymbol{u} \cdot \nabla(\boldsymbol{\sigma} - \boldsymbol{\sigma}_h) \rvert\rvert\rvert_{\tilde{\theta}}$	6.1279e-2	3.0111e-2	1.5208e-2	7.7004e-3	3.8803e-3
	Cvge. Rate	-	1.0	1.0	1.0	1.0

5.2 Example 2

For a second example the numerical approximation of viscoelastic flow through a planar 4:1 contraction channel is presented. This has been a long standing benchmark problem for viscoelastic flow [17, 20, 21]. A diagram of the flow geometry is given in Figure 5.2. It is assumed that the channel lengths are sufficiently long for fully developed Poiseuille flow at both the inflow and outflow boundaries. In the computations the value of L in Figure 5.2 is set at $1/4$.

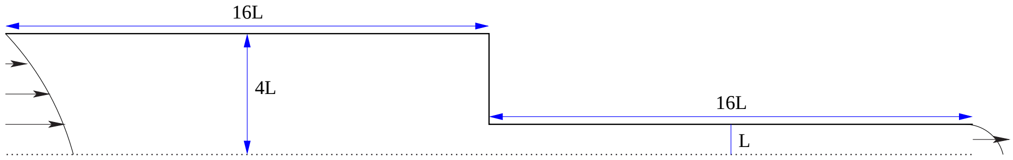

Figure 5.2: Plot of 4:1 contraction domain geometry.

The flow at $t = 0$ is assumed to be stationary and then slowly increased for $t > 0$ using $A(t) = 1 - e^{-t}$. The boundary conditions at the inflow of the channel are defined by

$$\boldsymbol{u} = A(t) \begin{pmatrix} \frac{1}{32}\left(1 - y^2\right) \\ 0 \end{pmatrix}, \tag{5.4}$$

and

$$\sigma_{11} = \frac{\lambda A(t)^2 y^2 \alpha(1+a)}{D(t)}, \quad \sigma_{12} = \frac{-16\alpha A(t) y}{D(t)}, \quad \text{and} \quad \sigma_{22} = \frac{\lambda A(t)^2 y^2 \alpha(a-1)}{D(t)}, \tag{5.5}$$

where

$$D(t) = 256 + A(t)^2 y^2 \lambda^2 (1+a)(1-a).$$

The outflow boundary condition is

$$\boldsymbol{u} = A(t) \begin{pmatrix} 2\left(\frac{1}{16} - y^2\right) \\ 0 \end{pmatrix}. \tag{5.6}$$

No slip boundary conditions were imposed for the velocity on the solid walls of the contraction, and a symmetry condition was imposed along the bottom of the computational domain. The computations were performed on a uniformly refined version of the mesh shown in Figure 5.3 with $\Delta x_{\min} = 0.0625$ and $\Delta y_{\min} = 0.015625$.

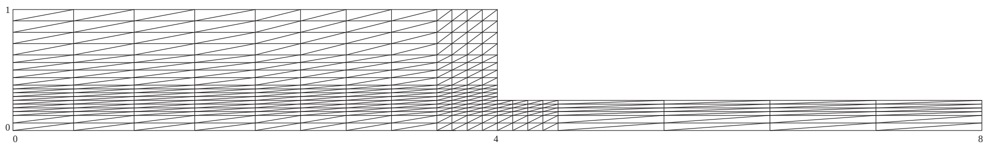

Figure 5.3: Sample Contraction Mesh

The computations were done using the full θ-method approximation given by (4.2) - (4.7) for an Oldroyd B fluid ($a = 1$), with $\lambda = 2$ and $Re = 1$. The value of α was set to $8/9$, which is commonly used in the literature [20]. The discrete time step and upwinding parameter were set to $\Delta t = 1/32$ and $\delta = (2/\Delta y_{\min})^2$. Figures 5.4 and 5.5 show streamlines for the fluid at times $t = 1/8, 1/2, 1$, and 4 superimposed on a contour plot showing the magnitude of velocity. Note that, consistent with expectations, as the velocity is increased, a vortex appears in the upper corner of the domain and grows with the magnitude of the velocity.

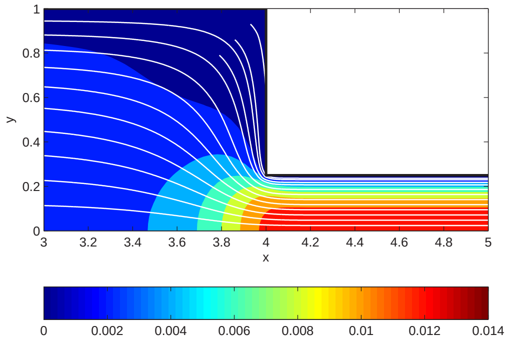

(a) $t = 0.125$

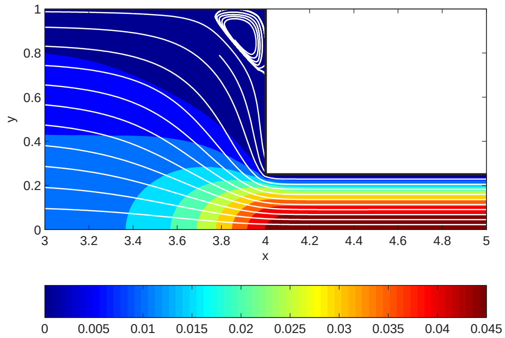

(b) $t = 0.5$

Figure 5.4: Streamlines and magnitude contours for $\boldsymbol{u}$

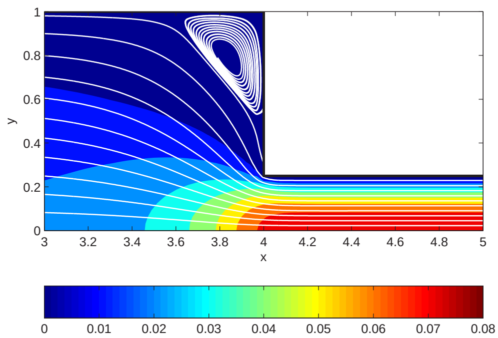

(a) $t = 1$

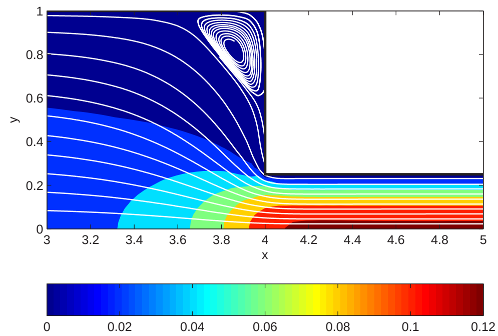

(b) $t = 4$

Figure 5.5: Streamline and magnitude contours for $\boldsymbol{u}$

References

[1] J. Baranger and A. Machmoum. Existence of approximate solutions and error bounds for viscoelastic fluid flow: characteristics method. *Comput. Methods Appl. Mech. Engrg.*, 148(1-2):39–52, 1997.

[2] J. Baranger and D. Sandri. Finite element approximation of viscoelastic fluid flow: existence of approximate solutions and error bounds. I. Discontinuous constraints. *Numer. Math.*, 63(1):13–27, 1992.

[3] J. Baranger and S. Wardi. Numerical analysis of a FEM for a transient viscoelastic flow. *Comput. Methods Appl. Mech. Engrg.*, 125(1-4):171–185, 1995.

[4] M. Bensaada and D. Esselaoui. Error estimates for a stabilized finite element method for the Oldroyd B model. *J. Math. Anal. Appl.*, 325(2):1042–1059, 2007.

[5] R.B. Bird, R.C. Armstrong, and O. Hassager. *Dynamics of Polymeric Liquids.* Fluid Mechanics. Wiley-Interscience, 1987.

[6] J.C. Chrispell, V.J. Ervin, and E.W. Jenkins. A fractional step θ-method for convection-diffusion using a SUPG approximation. Technical Report `TR2006_11_CEJ`, Clemson University, 2006.

[7] J.C. Chrispell, V.J. Ervin, and E.W. Jenkins. A fractional step θ-method for convection-diffusion problems. *J. Math. Anal. Appl.*, 333(1):204–218, 2007.

[8] J.C. Chrispell, V.J. Ervin, and E.W. Jenkins. A fractional step θ-method for viscoelastic fluid flow using a SUPG approximation. Technical Report `TR2007_10_CEJ`, Clemson University, 2007.

[9] V.J. Ervin and N. Heuer. Approximation of time-dependent, viscoelastic fluid flow: Crank-Nicolson, finite element approximation. *Numer. Methods Partial Differential Equations*, 20(2):248–283, 2004.

[10] V.J. Ervin and W.W. Miles. Approximation of time-dependent viscoelastic fluid flow: SUPG approximation. *SIAM J. Numer. Anal.*, 41(2):457–486 (electronic), 2003.

[11] E. Fernández-Cara, F. Guillén, and R.R. Ortega. Mathematical modeling and analysis of viscoelastic fluids of the Oldroyd kind. In *Handbook of Numerical Analysis, Vol. VIII*, pages 543–661. North-Holland, Amsterdam, 2002.

[12] R. Glowinski and J.F. Périaux. Numerical methods for nonlinear problem in fluid dynamics. In *Supercomputing*, pages 381–479. North-Holland, Amsterdam, 1987.

[13] C. Guillopé and J.-C. Saut. Existence results for the flow of viscoelastic fluids with a differential constitutive law. *Nonlinear Anal.*, 15(9):849–869, 1990.

[14] F. Hecht, O. Pironneau, A. Le Hyaric, and K. Ohtsuka. *FreeFem++*. http://www.freefem.org/ff++, 2005.

[15] V. John. *Large eddy simulation of turbulent incompressible flows*, volume 34 of *Lecture Notes in Computational Science and Engineering*. Springer-Verlag, Berlin, 2004. Analytical and numerical results for a class of LES models.

[16] P. Klouček and F.S. Rys. Stability of the fractional step θ-scheme for the nonstationary Navier-Stokes equations. *SIAM J. Numer. Anal.*, 31(5):1312–1335, 1994.

[17] J.M. Marchal and M.J. Crochet. Hermitian finite elements for calculating viscoelastic flow. *Journal of Non-Newtonian Fluid Mechanics*, 20:187–207, 1986.

[18] J.M. Marchal and M.J. Crochet. A new mixed finite element for calculation of viscoelastic flow. *Journal of Non-Newtonian Fluid Mechanics*, 26:77–114, 1987.

[19] S. Müller-Urbaniak. *Eine Analyse dex Zweischritt-θ-Verfahrens zur Lösung der instationären Navier-Stokes-Gleichungen.* PhD thesis, University of Heidelberg, 1994.

[20] R.G. Owens and T.N. Phillips. *Computational rheology.* Imperial College Press, London, 2002.

[21] T.N. Phillips and A.J. Williams. Viscoelastic flow through a planar contraction using a semi-lagrangian finite volume method. *Journal of Non-Newtonian Fluid Mechanics*, 87:215–246, 1999.

[22] M. Renardy. *Mathematical analysis of viscoelastic flows*, volume 73 of *CBMS-NSF Regional Conference Series in Applied Mathematics.* Society for Industrial and Applied Mathematics (SIAM), Philadelphia, PA, 2000.

[23] D. Sandri. Finite element approximation of viscoelastic fluid flow: existence of approximate solutions and error bounds. Continuous approximation of the stress. *SIAM J. Numer. Anal.*, 31(2):362–377, 1994.

[24] P. Saramito. A new θ-scheme algorithm and incompressible FEM for viscoelastic fluid flows. *RAIRO Modél. Math. Anal. Numér.*, 28(1):1–35, 1994.

[25] P. Saramito. Efficient simulation of nonlinear viscoelastic fluid flows. *J. Non-Newt. Fluid Mech.*, 60:199–223, 1995.

[26] R. Sureshkumar, M.D. Smith, R.C. Armstrong, and R.A. Brown. Linear stability and dynamics of viscoelastic flows using time-dependent numerical simulations. *J. Non-Newt. Fluid Mech.*, 82:57–104, 1999.

[27] S. Turek. A comparative study of time-stepping techniques for the incompressible Navier-Stokes equations: from fully implicit non-linear schemes to semi-implicit projection methods. *Internat. J. Numer. Methods Fluids*, 22(10):987–1011, 1996.

[28] S. Turek. *Efficient solvers for incompressible flow problems*, volume 6 of *Lecture Notes in Computational Science and Engineering.* Springer-Verlag, Berlin, 1999.